

An X-Ray Diffraction Study on the Structure of 18-Crown-6 Ether Complexes with Alkali Metal Ions in Aqueous Solution

Kazuhiko OZUTSUMI,[§] Masahiko NATSUHARA,[†] and Hitoshi OHTAKI*

Coordination Chemistry Laboratories, Institute for Molecular Science, Myodaiji, Okazaki 444

[†]Department of Electronic Chemistry, Tokyo Institute of Technology at Nagatsuta,

Nagatsuta-cho 4259, Midori-ku, Yokohama 227

(Received April 14, 1989)

The structure of 1,4,7,10,13,16-hexaoxacyclooctadecane (18-crown-6) and its complexes with alkali metal ions in aqueous solution has been investigated by X-ray diffraction and Raman spectroscopic methods at 25 °C. The X-ray scattering data and Raman spectrum for an aqueous 18-crown-6 solution show that free 18-crown-6 has a conformation of C_1 or D_{3d} symmetry. The molecule seems to be flexible and may be present as a mixture of the two conformations in aqueous solution. The structure of the lithium complex was not conclusive because of a weak scattering power of lithium atoms and weak complex formation between lithium ion and 18-crown-6. The sodium 18-crown-6 complex is estimated to have a structure similar to that found in crystal. The 18-crown-6 ring within the complex adopts the C_1 conformation, where five oxygen atoms within 18-crown-6 coordinate to sodium ion at the equatorial position and an oxygen atom within 18-crown-6 and a water molecule at the axial one. The structure of the potassium complex is also similar to that in crystal in which the D_{3d} conformation is taken. Potassium ion is located at the center of the mean plane of 18-crown-6 and one or two water molecules solvate potassium ion above and/or below the plane of 18-crown-6. It is suggested that the structure of the caesium complex is with either C_1 or D_{3d} symmetry, where caesium ion is apart from the mean plane of 18-crown-6. The rubidium complex was not examined because of a strong fluorescent X-ray emission from rubidium atoms when studied. The 18-crown-6 ring in the sodium and potassium complexes is rather rigid probably because the cavity of the ring well fits to the metal ions, while the ring coordinating to large caesium ion becomes more flexible than that in the sodium and potassium complexes due to weaker interaction with caesium ion.

Synthetic macrocyclic polyethers (crown ethers) can be good model compounds of ionophores such as nonactin and valinomycin in biological systems because of the similarity in structure and ion selectivity. Metal complexes with polyethers are also useful in organic syntheses since they increase the nucleophilic reactivity of halide ions by solubilizing metal halides in many organic solvents. In these respects, complexation equilibria of metal ions with crown ethers have extensively been investigated in various solvents.¹⁾ Many complexes with crown ethers have also been isolated and their structures in crystal have been determined.²⁾

It has been found that the conformational change of valinomycin occurs in the course of complexation with potassium ion in methanol.³⁾ Crown ethers seem to be similarly flexible in solution and thus the structure determined in crystal may sometimes be different from that in solution. The flexibility of the crown ring may play an important role in the complexation with metal ions. However, thermodynamic quantities of crown ether complexes in solution have been interpreted on the basis of their structures in crystal because of insufficient structural information of the complexes in solution. It has also been shown that the stability constants of crown ether complexes are strongly dependent on properties of solvents.⁴⁾ Solvation of the complexes is also an important factor for the stability and reactivity of the complexes as well

as the conformation of the ring structure in solution. Thus, we aimed at determining the structure of 1,4,7,10,13,16-hexaoxacyclooctadecane (18-crown-6) complexes with alkali metal ions, as well as the structure of the free ligand, in aqueous solution by employing X-ray diffraction and Raman spectroscopic methods in order to obtain more direct structural information in solution.

The structure of 18-crown-6⁴⁾ and its 1:1 complexes with monovalent cations^{5–13)} has been determined in crystal. Two ring oxygen atoms and two water molecules coordinate to lithium ion in the $\text{LiClO}_4 \cdot (18\text{-crown-6}) \cdot 2\text{H}_2\text{O}$ crystal.¹³⁾ Other cations are all coordinated with six oxygen atoms within 18-crown-6 and the seventh and/or eighth coordination sites of metal ions are occupied by anions in most complexes in crystal. The sites may, however, be occupied by solvent molecules in solution.

The most stable conformation of free 18-crown-6 in an isolated state was evaluated to be the one with C_1 symmetry from a molecular mechanical study,¹⁴⁾ and the conformation has also been found in the 18-crown-6 crystal.⁴⁾ On the other hand, in aqueous solution the most stable conformation is proposed to be with D_{3d} symmetry by the Monte Carlo simulation.¹⁵⁾ The different structures of the 18-crown-6 ether in solution and in crystal are due to solvation of the compound with water molecules in the former. The C_1 conformation was found in the NaSCN -18-crown-6 complex in crystal⁷⁾ and the D_{3d} conformation was observed in other 18-crown-6 complexes with monovalent cations including lithium ion.^{5,6,8–13)} The most

[§] Present address: Department of Chemistry, The University of Tsukuba, Tsukuba, Ibaraki 305.

Table 1. Structure of 18-Crown-6 and Its Complexes with Alkali Metal Ions Estimated by Various Methods

Form	Method	Free ligand	Lithium complex	Sodium complex	Potassium complex	Caesium complex
Crystal ^{a)}	X-Ray	C _i	D _{3d}	C ₁	D _{3d}	D _{3d}
Methanol ^{b)} solution	Raman	D _{3d}	—	D _{3d}	D _{3d}	D _{3d}
Isolated ^{c)} molecule	Molecular mechanics	C _i	—	C ₁	D _{3d}	D _{3d}
Aqueous ^{d)} solution	Monte Carlo simulation	D _{3d}	—	—	—	—

a) Refs. 4, 7, 8, 12, and 13. b) Ref. 18. c) Ref. 14. d) Ref. 15.

Table 2. Composition (mol dm⁻³), Stoichiometric Volumes *V*, and Densities ρ of the Sample Solutions

	A	B (M=Li)	C (M=Li)	D (M=Na)	E (M=K)	F (M=Cs)
MCl	—	1.503	1.996	2.023	1.942	1.508
18C6	2.007	1.805	2.105	2.213	1.991	1.832
H ₂ O	30.76	31.65	27.37	25.28	26.97	29.08
$\rho/\text{g cm}^{-3}$	1.085	1.111	1.134	1.159	1.157	1.262
$V/10^3 \text{ pm}^3$	0.8272	1.105	0.8320	0.8208	0.8551	1.101
C_{18C6}/C_M	—	1.201	1.055	1.094	1.025	1.215

stable conformation of 18-crown-6 within the sodium and potassium complexes in an isolated state without any hydrated water molecules was found to be C₁ and D_{3d}, respectively, by the molecular mechanical calculations.¹⁴⁾ It is suggested that the D_{3d} conformation is more stable than the C₁ conformation in the potassium complex with two water molecules coordinating to metal ions, while the energy difference between the C₁ and D_{3d} conformations was very small in the sodium complex according to the same method.¹⁴⁾ Thus it is seen that the solvation of 18-crown-6 greatly affects its conformation in solution. The structures of free 18-crown-6 and the complexes in various states reported so far by employing different methods are summarized in Table 1.

Although the conformation of 18-crown-6 in solution has so far been investigated by the dipole moment¹⁶⁾ and Raman spectral measurements,^{17,18)} no direct structural data of the solvated complexes have been given. An EXAFS measurement for the rubidium complex in solution has been carried out,¹⁹⁾ but the structure analysis is still incomplete. In the present paper we report the structural data of 18-crown-6 complexes with alkali metal ions, except rubidium ion, in aqueous solution studied by the X-ray diffraction method in order to obtain information on both conformation and solvation of the complexes. The structure of the rubidium complex was not determinable by the present method because of a strong fluorescent X-ray radiation. Raman spectroscopic measurements were also carried out to obtain additional information of the structure of the complexes.

Experimental

Preparation of Sample Solutions. NISSO 18-crown-6 (99%) was used without further purification and dried at room temperature under a reduced pressure. Alkali chlorides of reagent grade were recrystallized once from water.

Six sample solutions were prepared for the X-ray diffraction measurements. Solution A was an aqueous 18-crown-6 solution. Solutions B through F were prepared by dissolving alkali chlorides and 18-crown-6 in water. Concentrations of chloride ions in the test solutions were gravimetrically determined as AgCl. Concentrations of alkali metal ions in the solutions were evaluated from the stoichiometry of the salts used. Concentrations of 18-crown-6 were calculated from the weighted amounts of 18-crown-6. Densities of the solutions were measured by using pycnometer. The composition of the solutions is listed in Table 2.

X-Ray Scattering Measurements. X-Ray scattering measurements were performed on a JEOL θ - θ type diffractometer by using Mo $K\alpha$ radiation ($\lambda=71.07 \text{ pm}$). The method of measurements and data treatments were described elsewhere.²⁰⁾ The accessible range of scattering angle 2θ was from 2° to 140° , which corresponded to the scattering variable s ($=4\pi\lambda^{-1}\sin\theta$) range of 0.3×10^{-2} to $16.6\times 10^{-2} \text{ pm}^{-1}$. Times required to accumulate 80000 counts were recorded at each angle of 2θ and the measurement was repeated three times over the whole angle range.

The reduced intensities $i(s)$ were obtained by subtracting independent coherent scatterings from the measured intensities $I(s)$ as follows:

$$i(s) = KI(s) - \sum_j n_j [\{ f_j(s) + \Delta f_j' \}^2 + (\Delta f_j'')^2], \quad (1)$$

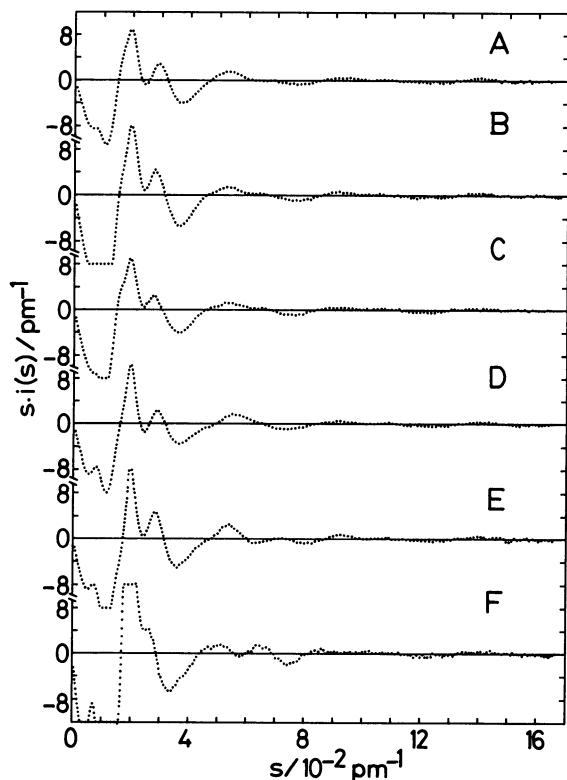


Fig. 1. The reduced intensities multiplied by s for solutions A through F.

where K stands for a normalization factor of the measured intensities to the absolute ones. n_j is the number of atom j in a stoichiometric volume V of the test solutions. $f_j(s)$ represents the atomic scattering factor at s , and $\Delta f'_j$ and $\Delta f''_j$ denote the real and imaginary parts of anomalous dispersion, respectively, of atom j . The reduced intensities multiplied by s for the sample solutions are shown in Fig. 1.

The radial distribution function $D(r)$ was calculated by the Fourier transform of the reduced intensities according to Eq. 2:

$$D(r) = 4\pi r^2 \rho_0 + \frac{2r}{\pi} \int_0^{s_{\max}} s \cdot i(s) \cdot M(s) \cdot \sin(rs) ds, \quad (2)$$

where ρ_0 ($=\{\sum n_j \cdot f_j(0)\}^2/V$) is the average scattering density in a stoichiometric volume of the sample solution and s_{\max} represents the maximum s -value attained in the measurement ($s_{\max}=16.6 \times 10^{-2} \text{ pm}^{-1}$). The modification function $M(s)$ is given as

$$M(s) = \frac{\sum_j n_j \{ (f_j(0) + \Delta f'_j)^2 + (\Delta f''_j)^2 \}}{\sum_j n_j \{ (f_j(s) + \Delta f'_j)^2 + (\Delta f''_j)^2 \}} \cdot \exp(-ks^2). \quad (3)$$

The damping factor k was chosen as 100 pm^2 in the present case. The $(D(r) - 4\pi r^2 \rho_0)$ curves for the test solutions are depicted in Fig. 2.

A least-squares calculation for the refinement of the structure parameters was applied to the reduced intensities so as to minimize the error-square sum U ,

$$U = \sum_{s_{\min}}^{s_{\max}} s^2 \{ i(s)_{\text{obsd}} - i(s)_{\text{calcd}} \}^2. \quad (4)$$

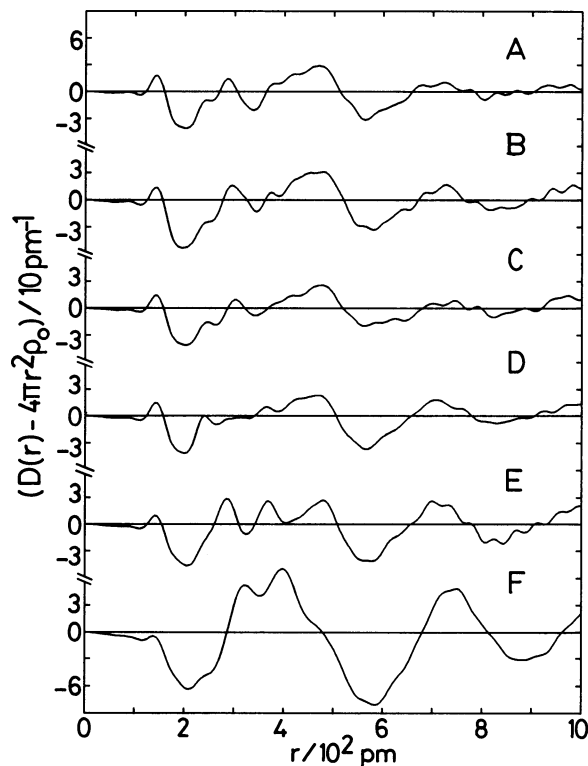


Fig. 2. The differential radial distribution curves, $D(r) - 4\pi r^2 \rho_0$, for solutions A through F.

The theoretical intensities $i(s)_{\text{calcd}}$ arising from the interatomic interactions in the solutions are obtained as follows:

$$i(s)_{\text{calcd}} = \sum_{\substack{p, q \\ p \neq q}} n_{pq} [\{f_p(s) + \Delta f'_p\} \{f_q(s) + \Delta f'_q\} + (\Delta f''_p)(\Delta f''_q)] \\ \times \frac{\sin(r_{pq}s)}{r_{pq}s} \cdot \exp(-b_{pq}s^2), \quad (5)$$

where r_{pq} , b_{pq} , and n_{pq} represent the distance, the temperature factor, and the frequency factor of the atom-pair p - q , respectively.

All calculations were performed by using programs KURVLR²¹ and NLPLSQ.²²

Raman Spectroscopic Measurements. Raman spectra for solutions A through F were measured by JEOL JRS-400T laser Raman spectrophotometer equipped with an Ar⁺ ion laser (Spectra-Physics Model 125 laser) using 514.5 nm excited line at the Instrumental Center of the Institute for Molecular Science.

Results and Discussion

Raman Spectra. Figure 3 shows the Raman spectra for solutions A through F. Conformations of C_i , C_1 , and D_{3d} symmetry have been known for the 18-crown-6 ring in the crystalline state. The C_i and C_1 conformations have been found in the crystals of pure 18-crown-6 and the NaSCN-18-crown-6 complex, respectively.^{4,7} The D_{3d} symmetry is observed in various metal complexes with 18-crown-6 in crys-

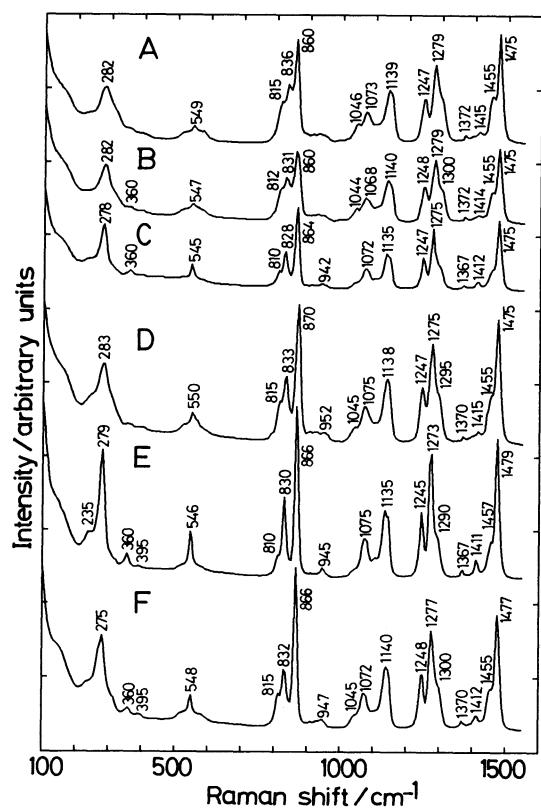


Fig. 3. The Raman spectra for solutions A through F.

tal.^{5,6,8-13}) The Raman spectrum of pure 18-crown-6 in the solid state which has the conformation of the C_i symmetry has been reported,^{17,18} in which strong bands appeared at 271, 320, 415, 580, 824, 868, 892, and 988 cm^{-1} . However, the bands at 320, 415, 580, 824, 892, and 988 cm^{-1} are not observed in the spectrum of the solution sample of free 18-crown-6 (see Fig. 3). On the other hand, the band at 549 cm^{-1} observed for the solution sample is not seen in the spectrum of the crystal having the C_i conformation. No Raman spectroscopic data are available for pure 18-crown-6 with other conformations in the solid state and no direct comparison may be possible between the spectrum of free 18-crown-6 in Fig. 3 and those of metal complexes, because coordination of the ligating atoms of the crown ring to metal ions usually strongly influences vibrational modes of the ligand molecule. It is thus conclusive from the Raman spectra that 18-crown-6 in solution has not the conformation of the C_i symmetry and probably it takes either C_1 or D_{3d} symmetry, or is present as a mixture of the two. This result agrees with the conclusion of the C_i conformation which is the least stable in aqueous solution according to the Monte Carlo simulation for the conformation of 18-crown-6.¹⁵⁾

The band at 550 cm^{-1} becomes sharper when an alkali metal ion is introduced in the ring (see Fig. 3, B–F).

Table 3. Interatomic Distances (r) below 500 pm and the Frequency Factors (n) of the Relevant Atom-Pairs within 18-Crown-6 of Different Conformations^{a)}

Interaction	r/pm				n
	C_i	C_1	D_{3d}		
C–H ($C_2\cdots H_1$)	106	106	106		24
C–O ($C_2\cdots O_1$)	142	142	142		12
C–C ($C_2\cdots C_3$)	151	151	151		6
O \cdots H ($O_1\cdots H_1$)	201	199	199		24
C \cdots H ($C_2\cdots H_3$)	209	206	205		24
C \cdots O ($C_3\cdots O_1$)	239	238	237		12
C \cdots C ($C_3\cdots C_5$)	236	238	235		6
O \cdots H ($O_4\cdots H_1$)	256	261	253		12
C \cdots H ($C_5\cdots H_3$)	265	268	258		24
O \cdots O ($O_1\cdots O_4$)	315	276	281		6
C \cdots C ($C_2\cdots C_5$)	356	350	366		12
C \cdots O ($C_5\cdots O_1$)	411	391	412		12
O \cdots O ($O_1\cdots O_7$)	522	423	485		6
C \cdots C ($C_2\cdots C_6$)	462	449	473		6
C \cdots O ($C_6\cdots O_1$)	488	453	499		12

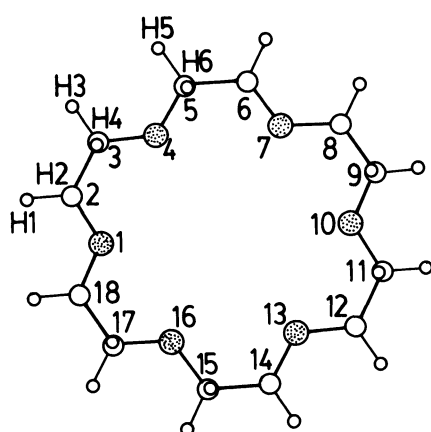
a) The distances are averaged ones.

A composite band around 860 cm^{-1} found in an aqueous 18-crown-6 solution (solution A) consists of two distinct bands at 836 and 860 cm^{-1} and a small peak at 815 cm^{-1} . The highest peak among the three, the band at ca. 860 cm^{-1} , shifts toward the high frequency side when an alkali metal ion is combined with the ligand. The order of the Raman shift is $\text{Li} < \text{Na} < \text{K} \approx \text{Cs}$, but it is not very clear when we take into account the uncertainty of the measurement ($\pm 2 \text{ cm}^{-1}$). However, the shape of the band at 860 cm^{-1} seems to be very closely related to the stabilities of the metal complexes,^{23,24} i.e., the sharpness of the peak changes in the order: free $< \text{Li} < \text{Na} < \text{K} > \text{Cs}$. The same trend can also be observed in the band shapes at ca. 280, 550, 1275, and 1475 cm^{-1} .

Radial Distribution Functions. 18-Crown-6 Solution. The radial distribution curve for an aqueous 18-crown-6 solution (solution A) is depicted in Fig. 2, A. Three large peaks appear around 140, 280, and 480 pm in the curve. In order to analyze the radial distribution function of solution A, intramolecular atomic distances for the conformations with C_i , C_1 , and D_{3d} symmetry are calculated from the structural data of 18-crown-6,⁴⁾ NaSCN–18-crown-6,⁷⁾ and KSCN–18-crown-6⁸⁾ crystals, respectively. The interatomic distances obtained from the data of RbSCN–18-crown-6¹¹⁾ and CsSCN–18-crown-6¹²⁾ crystals, in both of which the 18-crown-6 molecule adopts the D_{3d} conformation, are almost the same as those estimated from the structure of the KSCN–18-crown-6 crystal. The results are summarized in Table 3. For the sake of convenience in the following discussions, the atoms within an 18-crown-6 molecule are numbered as shown in Fig. 4.

From the table it is seen that the first peak at 140 pm is attributed to the C–H, C–O, and C–C bonds within 18-crown-6 molecules and the O–H bonds within

water molecules. The second peak at 280 pm with a shoulder at 240 pm includes peaks due to nonbonding intramolecular interactions such as $C_2 \cdots H_3$, $O_1 \cdots H_1$, $C_3 \cdots O_1$, $C_3 \cdots C_5$, $O_1 \cdots O_4$, $O_4 \cdots H_1$, and $C_5 \cdots H_3$ ones within 18-crown-6 molecules. Conformations of 18-crown-6 are very insensitive to the distances. It should be noted that the $C \cdots H$ and $O \cdots H$ interactions can not be neglected in the course of the analysis in spite of the weak scattering power of hydrogen atom, since the frequency factors for the interactions are very large (Table 3). The large peak around 480 pm is mainly due to various intramolecular interactions of



- Oxygen atom
- Carbon atom
- Hydrogen atom

Fig. 4. The numbering of atoms within 18-crown-6.

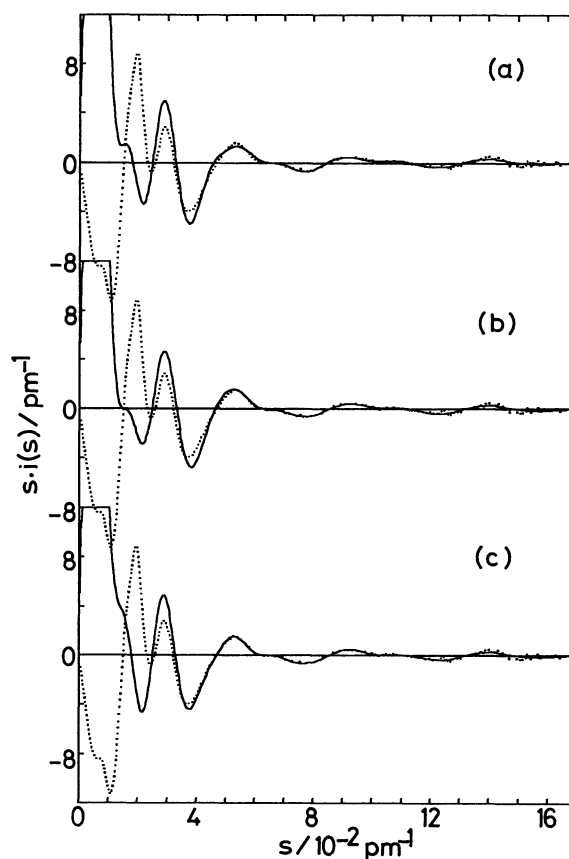


Fig. 5. The $s \cdot i(s)$ curve for solution A. The observed values are shown by the dotted lines and the calculated ones by assuming (a) C_i , (b) C_1 , and (c) D_{3d} conformations of 18-crown-6 are drawn by the solid lines.

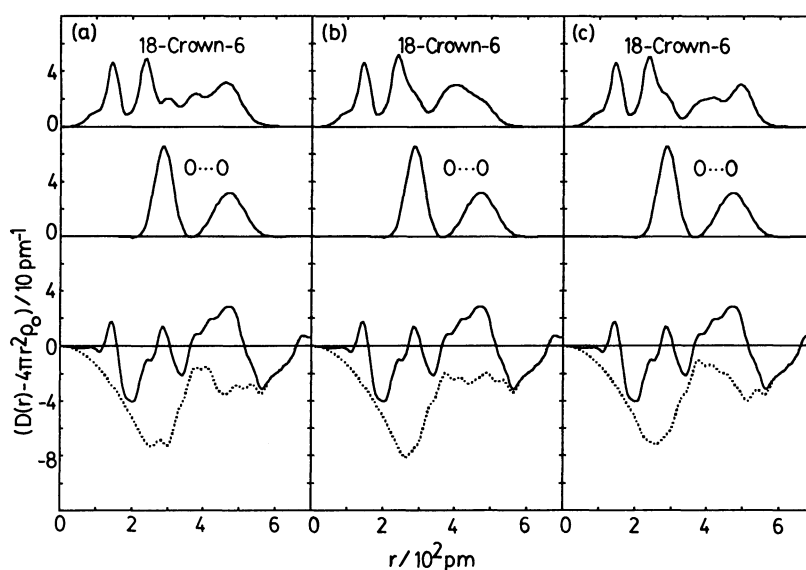


Fig. 6. The $(D(r) - 4\pi r^2 \rho_0)$ curve for solution A. The peak shapes for intramolecular interactions within 18-crown-6 are calculated on the basis of (a) C_i , (b) C_1 , and (c) D_{3d} conformations of 18-crown-6 (upper part). The dotted lines (lower part) represent the residual curves after subtraction of the theoretical peak shapes owing to the intramolecular interactions within 18-crown-6 and the $O \cdots O$ interactions of hydrated 18-crown-6 and of bulk water.

18-crown-6, the distances being varied depending on the conformations of 18-crown-6. The O...O interactions between water molecules in the bulk may appear also around 280 and 460 pm.²⁵⁾

In order to draw the theoretical reduced intensities and radial distribution curves by using the parameter values given in Table 3, the root mean square amplitudes Δr_{pq} of the atom-pairs were assumed to be 5% of the corresponding atom-pair distances, which have been evaluated from the results of solution X-ray diffraction measurements so far examined for non-bonding interatomic interactions which have a separation of one to two atoms in between. The temperature factors b_{pq} were thus calculated as $b_{pq} = (\Delta r_{pq})^2/2$. In the course of the calculations, hydration of oxygen atoms in 18-crown-6 was taken into account on the basis of the hydration model proposed by the Monte Carlo simulation.¹⁵⁾ The O...O contacts of bulk water were also considered.²⁵⁾ In Figs. 5 and 6 are shown the reduced intensities and radial distribution curves, respectively, thus calculated, all of which reasonably reproduce the experimental ones. Therefore, it is not conclusive which conformation predominantly exists in aqueous solution from the present X-ray scattering data, but the D_{3d} conformation (Fig. 5,C) seems to give the best fit result. According to the Raman spectroscopic measurement described in the preceding section, the C_i and D_{3d} conformations are possible to be present, and the C_1 conformation was not acceptable.

The peaks due to the intramolecular interactions of 18-crown-6 are large and comparable to those for O...O interactions of bulk water, and therefore, we must be careful to analyze peaks due to the intramolecular structure of 18-crown-6 complexes in the following sections with a reasonable evaluation of structure parameters for interactions between water molecules in the bulk, as well as those between atoms in the 18-crown-6 molecule.

LiCl and 18-Crown-6 Solutions. The $s \cdot i(s)$ (Figs. 1,B and C) and $(D(r) - 4\pi r^2 \rho_o)$ curves (Figs. 2,B and C) of aqueous LiCl solutions with 18-crown-6 (solutions B and C) are analyzed by the similar method to that employed for solution A. The C_i , C_1 , and D_{3d} conformations of 18-crown-6 were assumed at each calculation. As pointed out in the preceding section, complexation between lithium ion and 18-crown-6 was weak, and an only part of the whole lithium ions in the solution is trapped into the crown ring. In this calculation hydration of oxygen atoms in 18-crown-6 was not taken into consideration. The octahedral hydration model of chloride ion given in the literature was assumed.²⁶⁾ The Li-O interactions arising from the hydration of free lithium ion and from the complex between lithium ion and 18-crown-6 were neglected in the course of the calculation because of the weak scattering power of lithium atom and its low concentration in the solution. The results for solution

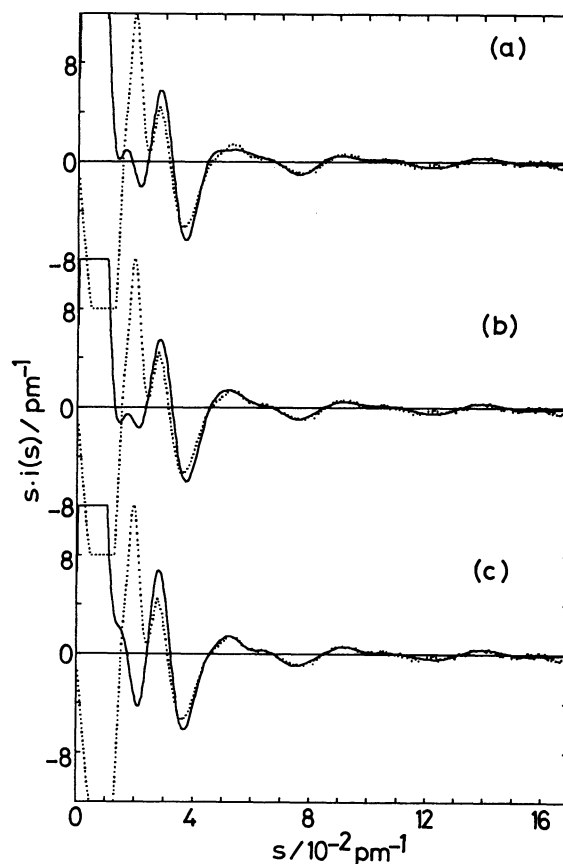


Fig. 7. The $s \cdot i(s)$ curve for solution B. The observed values are shown by the dotted lines and the calculated ones by assuming (a) C_i , (b) C_1 , and (c) D_{3d} conformations of 18-crown-6 are drawn by the solid lines.

B calculated by using different assumptions of the C_i , C_1 , and D_{3d} conformations are shown in Fig. 7 and practically the same results were also obtained for solution C. It may be rather difficult to draw a definite conclusion from the reduced intensities because all cases seem to give similar fits between experimental and calculated results. We may say that the D_{3d} symmetry (Fig. 7,C) gave the best fit result among the three, but this is not conclusive. The Raman spectroscopic data indicated that either the C_1 or D_{3d} conformation or both are possible for the lithium 18-crown-6 complex in solution (see Fig. 3).

NaCl and 18-Crown-6 Solution. The $(D(r) - 4\pi r^2 \rho_o)$ curve for solution D depicted in Fig. 2,D is also analyzed by assuming three structural models (C_i , C_1 , and D_{3d}) for the conformation of the 18-crown-6 ring in the sodium complex. In the C_i model sodium ion is located at the center of gravity of the six oxygen atoms in the ring and then is moved along the axis which is perpendicular to the mean plane defined by the six oxygen atoms in 18-crown-6. The position of sodium ion is determined so that the distance between the sodium ion and the nearest oxygen atom is ca. 245 pm,

which is estimated from the peak position in the radial distribution curve (Fig. 2,D). Two hydrated water molecules at the same distance from sodium ion are also taken into consideration in order to explain the peak area at ca. 245 pm. The 18-crown-6 ring in the sodium complex with thiocyanate ion as the counter anion in crystal has the C_1 conformation, i.e., sodium ion is surrounded by five oxygen atoms (O_1 to O_{13}) in the equatorial plane and an oxygen atom (O_{16}) and a water molecule coordinate at the axial site.⁷ For the D_{3d} conformation two model structures are examined: in one model sodium ion is located at the center of the six oxygen atoms within 18-crown-6 with D_{3d} symmetry, the structure corresponding to that found in KSCN-18-crown-6 crystal⁸ and, thus, the Na-O distance is ca. 280 pm. In the other model sodium ion contacts with two oxygen atoms at the distance of 240–250 pm in the mean plane of 18-crown-6. In both cases two hydrated water molecules above and below the plane are taken into consideration.

Among the structure models examined, the theoretical

values based on the C_1 model gave the best agreement with the experimental ones as shown in Fig. 8. The C_i and D_{3d} models do not fit to the observed curves. From these results we concluded that the structure of the sodium complex in aqueous solution is with the C_1 conformation which is similar to that in the solid state with one hydrated water molecule.

The structure parameters of the Na-18-crown-6 complex could not be well refined by a least-squares calculation using reduced intensities because of the low concentration of sodium ion and the relatively weak scattering power of sodium atom, since the contribution of intramolecular structure of 18-crown-6 to the intensity values is very large.

KCl and 18-Crown-6 Solution. The differential radial distribution curve for solution E (Fig. 2,E) shows two distinct peaks at 280 and 360 pm which are not observable in solutions A through D. The peaks may thus be ascribed to the K-O and K...C interactions within the K-18-crown-6 complex.

The $(D(r)-4\pi r^2 \rho_o)$ curve for solution E was

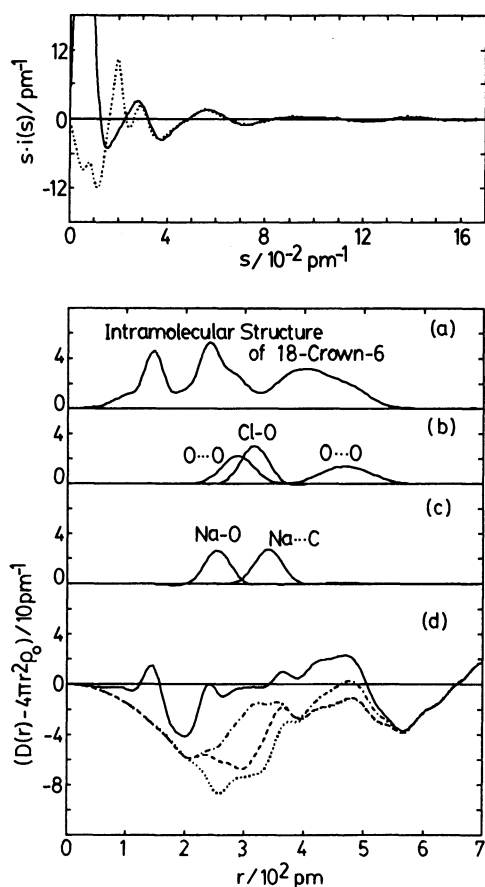


Fig. 8. The $s \cdot i(s)$ and $(D(r)-4\pi r^2 \rho_o)$ curves for solution D. The observed $s \cdot i(s)$ values are shown by the dotted line and calculated ones by the solid line (above). The observed radial distribution curve is drawn by the solid line, and chain, dashed, and dotted ones represent the residual curves after subtraction of calculated peak shapes in (a), (b), and (c), respectively (below).

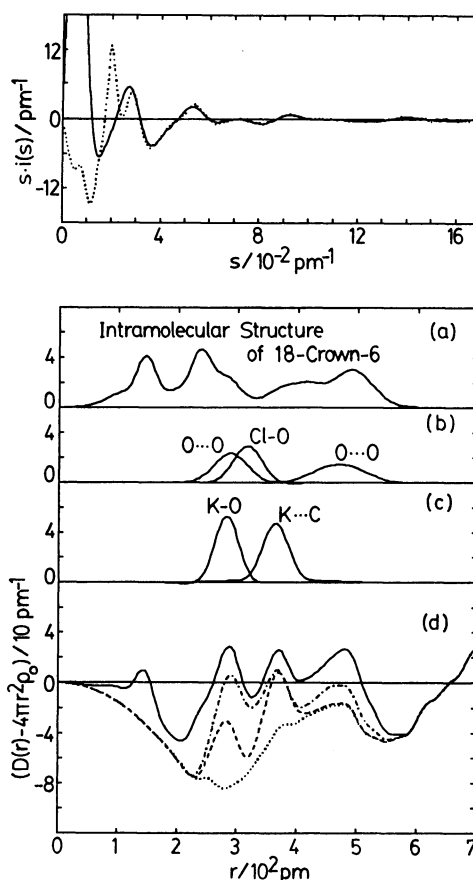


Fig. 9. The $s \cdot i(s)$ and $(D(r)-4\pi r^2 \rho_o)$ curves for solution E. The observed $s \cdot i(s)$ values are shown by the dotted line and calculated ones by the solid line (above). The observed radial distribution curve is drawn by the solid line, and chain, dashed, and dotted ones represent the residual curves after subtraction of calculated peak shapes in (a), (b), and (c), respectively (below).

analyzed in a similar manner to that employed in previous sections on the basis of three conformational models of 18-crown-6. For the C_i conformation, the same model as that employed for solution D was used. The distance between potassium ion and the nearest oxygen atom was taken to be ca. 280 pm. In the C_1 model potassium ion was moved along the line which is perpendicular to the mean plane defined by five oxygen atoms within 18-crown-6 through the center of gravity of these atoms, and in the course of this procedure, the K–O distance to the nearest oxygen atom within 18-crown-6 was assumed to be approximately 280 pm which were evaluated from the peak position in the $(D(r) - 4\pi r^2 \rho_o)$ curve. The conformation with D_{3d} symmetry was adopted which has been found in the KSCN–18-crown-6 crystal.⁸⁾ In all cases two water molecules bound to potassium ion at the distance of ca. 280 pm are taken into account. In these examinations the D_{3d} model gave the best-fit result. In Fig. 9 the reduced intensities and radial distribution curve drawn on the basis of the D_{3d} model are shown, in which theoretical curves well reproduced the experimental ones. Reduced intensity curves calculated from the C_i and C_1 models gave large discrepancies from the experimental ones. Thus the most plausible structure of the potassium complex was concluded to be the one with D_{3d} symmetry.

Since the contribution of interatomic interactions in 18-crown-6 and in the bulk water to the reduced intensities and radial distribution curve becomes almost comparable to those of K–O and K...C interactions (see Fig. 9), the direct analysis of the curve for the structural parameters of the K–O and K...C interactions may be largely affected by the assumption for the Cl–O distance and the hydration number of chloride ion in aqueous solution, which has been reported to be concentration dependent,²⁷⁾ as well as for the interatomic interactions in 18-crown-6 and in the bulk water. Therefore, the structure parameters for the potassium 18-crown-6 complex were evaluated by the following procedure: we first subtracted the reduced intensities for solution C containing 2 mol dm⁻³ lithium chloride, in which almost the same concentrations of 18-crown-6, chloride ion, and water molecule as in solution E are contained, from those of solution E. By this procedure the short-range interatomic interactions in 18-crown-6 below 300 pm, hydrated chloride ions and the bulk water, except for those of the metal–oxygen interactions, were eliminated. The contribution of long-range interatomic interactions in 18-crown-6 would entirely be eliminated when the conformation of 18-crown-6 in the potassium complex was the same as that in the lithium complex. Even if their conformations are different, the difference in the long-range interatomic interactions may be small enough to obtain the structure parameters for the potassium complex with a reasonable accuracy,

because the contribution of K–O and K...C interactions to the difference reduced intensities $\Delta\{s \cdot i(s)\}$ is much larger. The Li–O and Li...C interactions in case of solution C may be neglected because of the weak scattering power of lithium atom. The difference reduced intensities $\Delta\{s \cdot i(s)\}$ and difference radial distribution curve $\Delta D(r)$ are shown in Fig. 10. The $\Delta D(r)$ curve shows two distinct peaks at 278 and 360 pm which should be due to the K–O and K...C interactions, respectively. The areas under the peaks correspond to ca. seven K–O bonds and ca. twelve K...C interactions.

A least-squares calculation was finally applied to the $\Delta\{s \cdot i(s)\}$ curve in the high-angle region to optimize the structural parameters of the potassium 18-crown-6 complex. The conformation of 18-crown-6 within the potassium complex was assumed to be D_{3d} on the basis of the analysis of the radial distribution curve in the course of the refinements. Two types of the calculations were performed in the refinements: in the type I calculation, the conformation of 18-crown-6 in solution C was assumed to be the same as that in

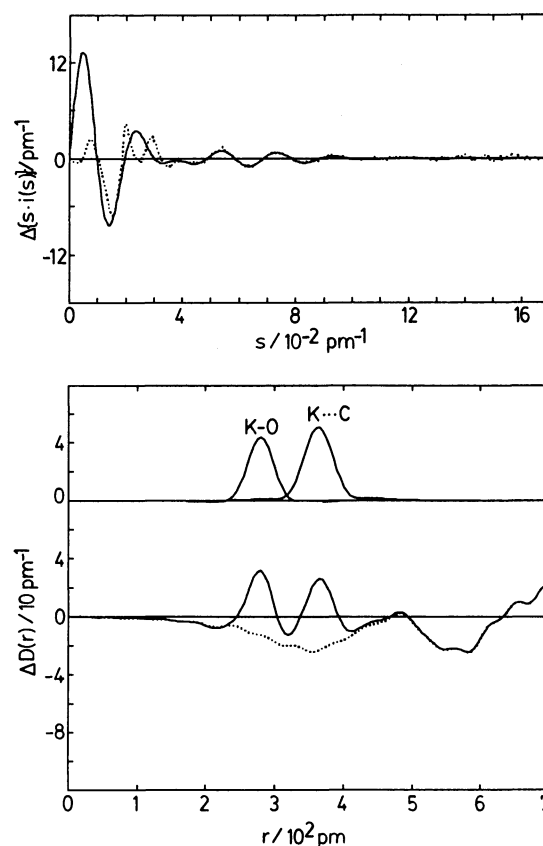


Fig. 10. The difference reduced intensities $\Delta\{s \cdot i(s)\}$ and difference radial distribution curve $\Delta D(r)$ for solution E. The observed $\Delta\{s \cdot i(s)\}$ values are shown by the dotted line and calculated ones by the solid line (above). The observed $\Delta D(r)$ curve is drawn by the solid line and the residual curve after subtraction of calculated peak shapes by the dotted line (below).

Table 4. Least-Squares Refinements for the Structure Parameters of the Potassium 18-Crown-6 Complex in Aqueous Solution with Different Models

Interaction	Parameter	I	II	Proposed length
K-O	r/pm	278(1)	276(1)	277(2)
	$b/10^2 \text{ pm}^2$	6(1)	12(2)	
	n	5.5(4)	8.2(6)	
K...C	r/pm	363(1)	356(1)	360(4)
	$b/10^2 \text{ pm}^2$	14(1)	14(1)	
	n	12 ^a	12 ^a	
	U/pm^{-2}	4.9	5.1	

a) The values were kept constant during the calculation.

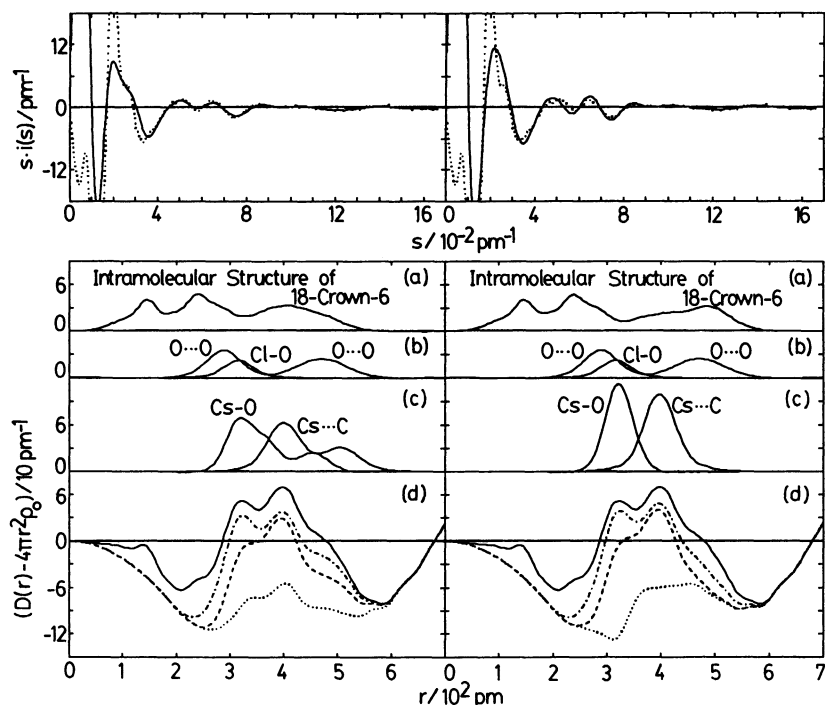


Fig. 11. The $s \cdot i(s)$ and $(D(r) - 4\pi r^2 \rho_0)$ curves for solution F. The theoretical curves are calculated on the basis of the C_1 (left) and D_{3d} (right) conformations. The observed $s \cdot i(s)$ values are shown by the dotted line and calculated ones by the solid line (above). The observed radial distribution curve is drawn by the solid line, and chain, dashed, and dotted ones represent the residual curves after subtraction of calculated peak shapes in (a), (b), and (c), respectively (below).

solution E (D_{3d} conformation). On the other hand, in the type II treatment, the conformations of 18-crown-6 in solutions C and E were different, the former 18-crown-6 adopting the C_1 conformation, and hence the structural difference between the two complexes must be taken into consideration. The results are summarized in Table 4 and very similar results were obtained by both treatments. The structural difference between lithium and potassium complexes did not thus affect the structure determination of the potassium complex even if their structures were different. The K-O and K...C distances determined are 277(2) and 360(4) pm, respectively, and therefore, potassium ion is located at the center of 18-crown-6. The frequency factor for the K-O bond is estimated to be 6–8, which suggests that

one or two water molecules solvate potassium ion above and/or below the mean plane of 18-crown-6 with D_{3d} symmetry.

CsCl and 18-Crown-6 Solution. The $(D(r) - 4\pi r^2 \rho_0)$ curve for solution F depicted in Fig. 2,F shows two large peaks around 310 and 390 pm. The peaks are assignable to the Cs-O and Cs...C interactions within the caesium 18-crown-6 complex.

The radial distribution function for solution F was analyzed by a similar procedure to that employed for solution E. The Cs-O distance to the nearest oxygen atom within 18-crown-6 was set to be 315 pm in the three models examined (C_i , C_1 , and D_{3d} models). Two water molecules with the same distance from the caesium ion were also taken into consideration in

order to explain the large area under the peak at 310 pm. Among the structure models examined, both C_1 and D_{3d} models rather reasonably reproduced the experimental values as depicted in Fig. 11. Therefore, it is not conclusive from the result which conformation is taken in the complex. Both can also exist as a mixture of two type conformations in the solution. The latter explanation seems to be likely because Cs–O interactions are rather weak and the Raman bands in the CsCl–18-crown-6 solution are broader than those of KCl–18-crown-6 solution.

The refinement of the structure parameters for the Cs–O and Cs...C interactions within the caesium complex was also performed by the similar method to that applied to the case of the potassium complex. In this case the reduced intensities of solution B were subtracted from those of solution F because the composition of the two solutions is very similar. The difference reduced intensities $\Delta\{s \cdot i(s)\}$ and difference radial distribution curve $\Delta D(r)$ are shown in Fig. 12. In the observed $\Delta D(r)$ curve two large broad peaks are found around 320 and 400 pm owing to the Cs–O and Cs...C interactions, respectively, which are less separated than those for the potassium complex. This suggests that the temperature factors for both Cs–O and Cs...C interactions are larger than those of K–O and K...C interactions. The large temperature factors of the

Cs–O and Cs...C pairs certainly arise from their weak interactions, and thus the Cs–O and Cs...C distances may fluctuate to a relatively large extent. In the crystal of CsSCN–18-crown-6 each of the Cs–O and Cs...C distances can be divided into two groups, i.e., three shorter Cs–O distances of 306 pm and three longer ones of 324 pm, and five shorter Cs...C distances of 377 pm and seven longer ones of 398 pm.¹²⁾ Therefore, we tried to separate the peaks in the radial distribution curve into four major ones on the basis of the crystallographic data. However, any combination of the interatomic distances and temperature factors was not successful to reproduce the experimental curves by using four kinds of interactions. Three different Cs–O bonds and two different Cs...C interactions, at least, were needed in order to explain the experimental result according to the least-squares calculations for the $\Delta\{s \cdot i(s)\}$ values when we adopted the C_1 conformation of the 18-crown-6 structure. On the other hand, only two interactions, one Cs–O and one Cs...C, were sufficient to interpret the difference reduced intensities of the solution on the basis of the D_{3d} symmetry model (see Table 5).

The structure parameters finally refined by a least-squares calculation using the high-angle region of the $\Delta\{s \cdot i(s)\}$ values are summarized in Table 5. Both models almost equally reproduce the experimental

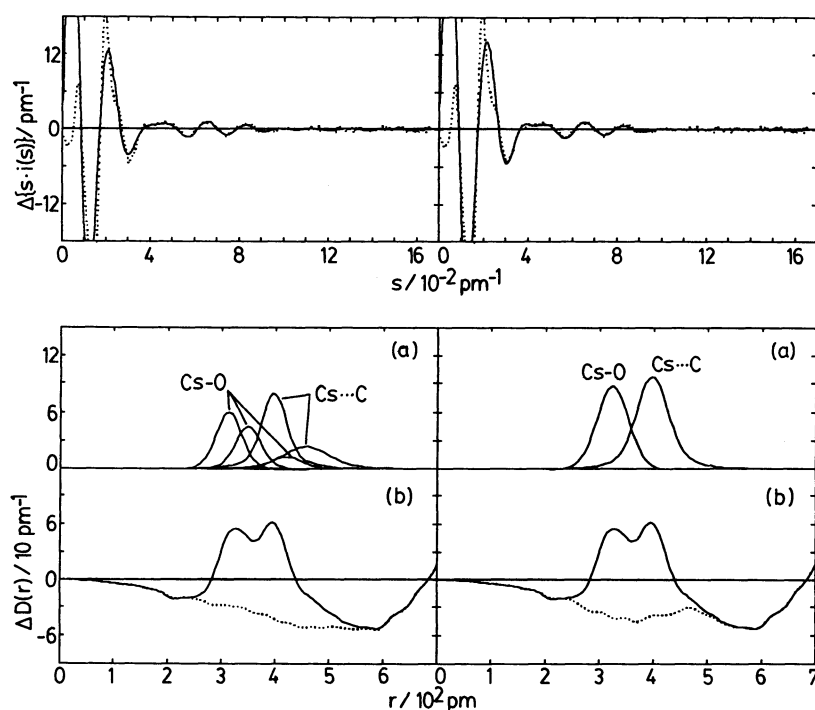


Fig. 12. The difference reduced intensities $\Delta\{s \cdot i(s)\}$ and difference radial distribution curve $\Delta D(r)$ for solution F. The theoretical curves are calculated on the basis of the C_1 (left) and D_{3d} (right) conformations. The observed $\Delta\{s \cdot i(s)\}$ values are shown by the dotted line and calculated ones by the solid line (above). The observed $\Delta D(r)$ curve is drawn by the solid line and the residual curve after subtraction of calculated peak shapes by the dotted line (below).

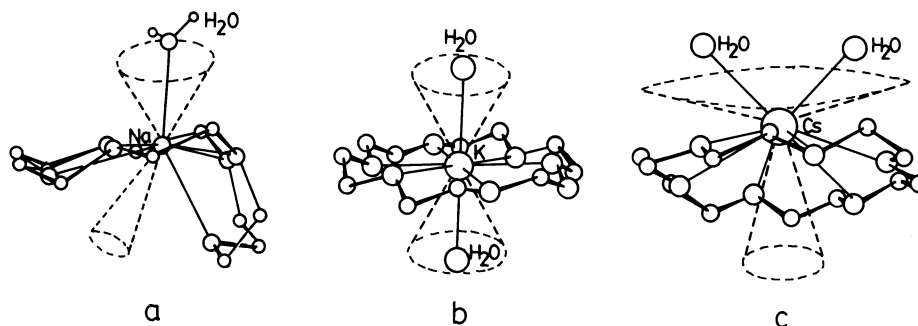


Fig. 13. Proposed structures of hydrated 18-crown-6 alkali metal complexes. Broken lines indicate corn angles above and below the metal ion in the complexes. (a) Sodium complex with C_1 conformation of the 18-crown-6 ring, (b) Potassium complex with D_{3d} conformation, (c) One of the possible structure of the caesium complex which has the D_{3d} conformation.

Table 5. Least-Squares Refinements for the Structure Parameters of the Caesium 18-Crown-6 Complex in Aqueous Solution with Different Models of the Crown-Ring Structure

Interaction	Parameter	C_1	D_{3d}
Cs-O	r/pm	312(2)	321(1)
	$b/10^2 \text{ pm}^2$	13(2)	27(4)
	n	4 ^{a, b)}	7.1(4)
Cs-O	r/pm	348(5)	—
	$b/10^2 \text{ pm}^2$	13(5)	—
	n	3 ^{a)}	—
Cs-O	r/pm	419(43)	—
	$b/10^2 \text{ pm}^2$	25 ^{a)}	—
	n	1 ^{a)}	—
Cs...C	r/pm	396(3)	394(1)
	$b/10^2 \text{ pm}^2$	15(4)	29(2)
	n	8 ^{a)}	12 ^{a)}
Cs...C	r/pm	453(20)	—
	$b/10^2 \text{ pm}^2$	71(54)	—
	n	4 ^{a)}	—
	$U/10 \text{ pm}^{-2}$	1.1	1.2

a) The values were kept constant during the calculation. b) The value was varied from 2 to 6 but practically the same Cs-O and Cs...C distances were obtained.

curve. Therefore it is concluded that Cs-18-crown-6 complex with different conformations C_1 and D_{3d} can be present, and the Cs-18-crown-6 complex takes either C_1 or D_{3d} conformation, or has a structure of their mixture in the solution. Since a large caesium ion cannot accommodate in the hole of the 18-crown-6 ring and is located apart from the mean plane of the ring, the ring may be more flexible than that in the sodium and potassium complexes, in which these ions are kept at the center of the ring, and thus, the latter explanation (mixture model) cannot be rejected from the conclusion. Since the frequency factor for the Cs-O bond in the D_{3d} model converged to 7.1(4), the caesium ion may be solvated with one to two water molecules in the solution.

In Fig. 13 plausible structures are depicted for the alkali metal complexes with 18-crown-6 in aqueous solution examined, except for the lithium complex whose structure was not estimated from the present work. Broken lines in the figure indicate corn angles around the central metal ions which are drawn by taking into account the van der Waals radii of oxygen, carbon, and hydrogen atoms in the 18-crown-6 ring. It is seen from the corn angles, it may be possible that only one water molecule combines with sodium ion in the complex. In the potassium complex, two water molecules can approach the central ion. For the caesium complex, about two water molecules can interact with caesium ion from one side of the crown ring.

The work has been financially supported by the Grant-in-Aid for Scientific Research No. 63612005 (Macromolecular Complexes) from the Ministry of Education, Science and Culture. Computer calculations were carried out at the computer center of the Institute for Molecular Science in Okazaki.

References

- 1) R. M. Izatt, J. S. Bradshaw, S. A. Nielsen, J. D. Lamb, J. J. Christensen, and D. Sen, *Chem. Rev.*, **85**, 271 (1985).
- 2) M. R. Truter, *Structure and Bonding*, **16**, 71 (1973).
- 3) D. J. Patel, *Biochemistry*, **12**, 496 (1973).
- 4) J. D. Dunitz and P. Seiler, *Acta Crystallogr., Sect. B*, **30**, 2739 (1974); E. Maverick, P. Seiler, W. B. Schweizer, and J. D. Dunitz, *Acta Crystallogr., Sect. B*, **36**, 615 (1980).
- 5) J.-P. Behr, P. Dumas, and D. Moras, *J. Am. Chem. Soc.*, **104**, 4540 (1982).
- 6) O. Nagano, A. Kobayashi, and Y. Sasaki, *Bull. Chem. Soc. Jpn.*, **51**, 790 (1978).
- 7) M. Dobler, J. D. Dunitz, and P. Seiler, *Acta Crystallogr., Sect. B*, **30**, 2741 (1974).
- 8) P. Seiler, M. Dobler, and J. D. Dunitz, *Acta Crystallogr., Sect. B*, **30**, 2744 (1974).
- 9) O. Nagano, *Acta Crystallogr., Sect. B*, **35**, 465 (1979).

- 10) O. Nagano and Y. Sasaki, *Acta Crystallogr., Sect. B*, **35**, 2387 (1979).
 - 11) M. Dobler and R. P. Phizackerley, *Acta Crystallogr., Sect. B*, **30**, 2746 (1974).
 - 12) M. Dobler and R. P. Phizackerley, *Acta Crystallogr., Sect. B*, **30**, 2748 (1974).
 - 13) P. Groth, *Acta Chem. Scand., Ser. A*, **36**, 109 (1982).
 - 14) G. Wipff, P. Weiner, and P. A. Kollman, *J. Am. Chem. Soc.*, **104**, 3249 (1982); G. Wipff, P. A. Kollman, and J. M. Lehn, *J. Mol. Struct.*, **93**, 153 (1983).
 - 15) G. Ranghino, S. Romano, J. M. Lehn, and G. Wipff, *J. Am. Chem. Soc.*, **107**, 7873 (1985).
 - 16) R. Perrin, C. Decoret, G. Bertholon, and R. Lamartine, *Nouv. J. Chim.*, **7**, 263 (1983).
 - 17) H. Sato and Y. Kusumoto, *Chem. Lett.*, **1978**, 635.
 - 18) H. Takeuchi, T. Arai, and I. Harada, *J. Mol. Struct.*, **146**, 197 (1986).
 - 19) J. Goulon and C. Goulon-Ginet, *Pure Appl. Chem.*, **54**, 2307 (1982).
 - 20) H. Ohtaki, *Rev. Inorg. Chem.*, **4**, 103 (1982).
 - 21) G. Johansson and M. Sandström, *Chem. Scr.*, **4**, 195 (1973).
 - 22) T. Yamaguchi, Doctor Thesis, Tokyo Institute of Technology, March (1978).
 - 23) H. K. Frensdorff, *J. Am. Chem. Soc.*, **93**, 600 (1971).
 - 24) R. M. Izatt, R. E. Terry, B. L. Haymore, L. D. Hansen, N. K. Dalley, A. G. Avondet, and J. J. Christensen, *J. Am. Chem. Soc.*, **98**, 7620 (1976).
 - 25) A. H. Narten, *ORNL-4578* (1970).
 - 26) G. Pálinkás, T. Radnai, and F. Hajdu, *Z. Naturforsch., A*, **35**, 107 (1980).
 - 27) T. Yamaguchi, H. Ohtaki, E. Spohr, G. Pálinkás, K. Heinzinger, and M. M. Probst, *Z. Naturforsch., A*, **41**, 1175 (1986).
-